ORIGINAL PAPER

Nagoya J. Med. Sci. **87**. 431–450, 2025
doi:10.18999/nagjms.87.3.431

XXYLT1 inhibits NOTCH1 activation in Jurkat cells while promoting cell proliferation

Weiwei Wang[1,2], Wataru Saiki[1,2], Yohei Tsukamoto[1,2,3], Sae Uchiyama[1,2], Yuji Kondo[1,2,4], Tetsuya Okajima[1,2,4] and Hideyuki Takeuchi[1,2,5]

[1]*Department of Molecular and Cellular Biology, Nagoya University Graduate School of Medicine, Nagoya, Japan*
[2]*Department of Molecular Biochemistry, Nagoya University Graduate School of Medicine, Nagoya, Japan*
[3]*Now with Department of Biochemistry, School of Pharmaceutical Sciences, University of Shizuoka, Shizuoka, Japan*
[4]*Institute for Glyco-Core Research (iGCORE), Nagoya University, Nagoya, Japan*
[5]*Department of Biochemistry, School of Pharmaceutical Sciences, University of Shizuoka, Shizuoka, Japan*

ABSTRACT

Glycosylation, a key post-translational modification, regulates protein function in many contexts. Epidermal growth factor-like repeats undergo domain-specific *O*-glycosylation such as *O*-glucosylation, *O*-fucosylation, and *O*-GlcNAc'ylation. *O*-Glucose glycans are attached to specific serine residues by the action of protein *O*-glucosyltransferase 1 (POGLUT1) and can be elongated with two xylose residues by glucoside α1-3xylosyltransferase 1 (GXYLT1) or glucoside α1-3xylosyltransferase 2 (GXYLT2) and xyloside α1-3xylosyltransferase 1 (XXYLT1) in mammals. The xylosyl elongation of *O*-glucose as a negative regulator of Notch in *Drosophila* has recently been reported, but its role in mammalian Notch signaling remains elusive. Here, we investigated the impact of terminal xylosylation by XXYLT1 on NOTCH1 signaling in Jurkat cells, a T-cell acute lymphoblastic leukemia cell line with cell-autonomous NOTCH1 activation due to the juxtamembrane expansion mutation. Mass spectrometry analysis of NOTCH1 fragments overexpressed in Jurkat cells demonstrated that the *O*-glucose site on NOTCH1 EGF10 was modified with various elongating patterns of *O*-glucose. Genetic deletion of *XXYLT1* in Jurkat cells led to enhanced activation of NOTCH1, suggesting that *XXYLT1* inhibited NOTCH1 activation in Jurkat cells, whereas the cell surface expression of NOTCH1 was not altered. Unexpectedly, the proliferation of Jurkat cells was impaired in *XXYLT1* knockout cells, with accompanying *MYC* downregulation, a Notch target gene. Our results revealed for the first time that mammalian Notch activation is fine-tuned by xylosylation in Jurkat cells, thus highlighting the potential of Notch agonism by the inhibition of xylosylation. Additionally, our findings regarding cell proliferation underscore the notion that there are possibly substrates other than NOTCH1 that XXYLT1 modifies, thereby regulating their functions in Jurkat cells.

Keywords: notch signaling, *O*-glucose, XXYLT1, T-ALL, Jurkat cells

Abbreviations:
EGF: epidermal growth factor-like
POGLUT1: protein *O*-glucosyltransferase 1
Xyl: xylose
XXYLT1: xyloside α1-3xylosyltransferase 1

Received: October 2, 2024; Accepted: December 2, 2024
Corresponding Author: Hideyuki Takeuchi, PhD
Department of Biochemistry, School of Pharmaceutical Sciences, University of Shizuoka,
52-1 Yada, Suruga-ku, Shizuoka 422-8526, Japan
Tel: +81-54-264-5725, E-mail: htakeuchi@u-shizuoka-ken.ac.jp

T-ALL: T-cell acute lymphoblastic leukemia
FBS: fetal bovine serum
PCR: polymerase chain reaction
Cas9: clustered regularly interspaced short palindromic repeats (CRISPR)-associated protein 9
KO: knockout

INTRODUCTION

Significant roles for post-translational modifications, including glycosylation, have been described in many contexts, including the modulation of signal transduction.[1-4] The Notch signaling pathway is an evolutionarily conserved cell-to-cell communication pathway that plays critical roles in cell fate decisions in metazoans. The roles of epidermal growth factor-like (EGF) domain-specific *O*-linked glycans in the extracellular domain of Notch receptors have been described for more than two decades.[5-8] *O*-Glucose (Glc), *O*-fucose (Fuc), and *O*-*N*-acetylglucosamine (GlcNAc) glycans are added to Notch EGF repeats as monosaccharides and can be further elongated with other sugar residues. Both *O*-Fuc and *O*-Glc are essential for Notch activation.[9-13] Additionally, recent extensive analyses have demonstrated that elongation of *O*-Fuc modulates Notch-ligand interactions, thereby affecting Notch activation.[14-17] However, the impact of the extension of *O*-Glc glycans remains elusive. In mammals, the classical *O*-Glc glycans are added by the action of protein *O*-glucosyltransferase 1 (POGLUT1, rumi in *Drosophila*) and extended with two xylose (Xyl) residues to a linear trisaccharide form (Xyl-α1,3-Xyl-α1,3-Glc-β1-*O*-Ser) by the sequential action of glucoside α1-3xylosyltransferase 1 or 2 (GXYLT1 or GXYLT2, shams in *Drosophila*) and xyloside α1-3xylosyltransferase 1 (XXYLT1, xxylt in *Drosophila*).[11,12,18-21] In flies, xylosyl elongation negatively regulates Notch activation by modulating Notch-Delta interactions in a specific context.[22-24] Recently, we reported that XXYLT1 in HEK293T cells promotes the cell surface presentation of NOTCH1 and NOTCH2 when overexpressed.[25] However, whether Notch xylosylation alters mammalian Notch activation remains unclear.

The aberrant activation or inactivation of Notch leads to various diseases, including cancers.[26] T-cell acute lymphoblastic leukemia (T-ALL) is closely related to NOTCH1, as over 60% of T-ALL cases possess activation mutations in *NOTCH1*.[27] Several classes of NOTCH1-activating mutations have been proposed.[28] Mutations in the heterodimerization domain (HD) or mutations that expand the juxtamembrane region of the extracellular domain of NOTCH1 result in autonomous exposure of site-2 (S2) where cleavage by extracellular metalloproteases such as ADAM10 or ADAM17 occurs, ultimately leading to site-3 (S3) cleavage by gamma-secretase that provokes ligand-independent and constitutive activation of NOTCH1.[29,30]

As previous studies have indicated that POGLUT1/Rumi is required for S2/S3 cleavages of Notch,[11,12] T-ALL appears to be a suitable context to clarify whether XXYLT1 acts in an opposite manner to POGLUT1 in the context of NOTCH1 signaling. Here, we investigated the contribution of *XXYLT1* in Jurkat cells, a T-ALL cell line with a juxtamembrane expansion mutation on *NOTCH1* that exhibits ligand-independent NOTCH1 activation[31] and report that *XXYLT1* inhibits NOTCH1 activation in Jurkat cells while promoting cell proliferation.

MATERIALS AND METHODS

Cell culture

Jurkat cells were a generous gift from Dr Koichi Furukawa of Chubu University. Jurkat cells were cultured in RPMI 1640 medium that was supplemented with 10% or 5% fetal bovine serum (FBS), 1 mM sodium pyruvate (Thermo Fisher Scientific, Waltham, MA, USA), 2 mM GlutaMAX (Thermo Fisher Scientific), 100 U/mL penicillin, and 100 μg/mL streptomycin. The cells were maintained at 37 °C in a humidified atmosphere containing 5% CO_2. HEK293T cells were cultured in a Dulbecco's Modified Eagle Medium (DMEM)-high glucose supplemented with 5% FBS, 100 U/mL penicillin, and 100 μg/mL streptomycin.

Plasmids

The expression plasmid encoding mouse NOTCH1 EGF8-12 with C-terminal Myc and His_6 tags was generated by polymerase chain reaction (PCR) amplification using KOD-FX-Neo polymerase (TOYOBO, Osaka, Japan), primers: 5′-ATATATAAGCTTTAGATGTGGACGAAT GTCAGCTC-3′ and 5′-ATCTAGCTCGAGCGATTTCACAGTATACACCTTCATAACCTG-3′, and pSectag2c/hygro-mouse NOTCH1-EGF1-36-MycHis_6 as template.[25] The PCR product was digested with Hind III and Xho I and ligated into the pSectag2c/hygro plasmid (Invitrogen). The lentivirus vector encoding human XXYLT1 with C-terminal HA tag was created by PCR amplification using KOD-FX-Neo polymerase, primers: 5′-ATATATCTCGAGATTCATGGGCCTCCTCCG-3′ and 5′-ATCTAGGAATTCCTCACAGGCTGGCGTAATC-3′ and pcDNA3.1(+)-FLAG-human XXYLT1-HA plasmid[19] as template. The PCR product was digested with XhoI and EcoRI and ligated into the pLVX-M-puro vector, a gift from Boyi Gan (Addgene plasmid, #125839; http://n2t.net/addgene, 125839; RRID, Addgene_125839).[32] The lentiviral packaging plasmid psPAX2 was a gift from Didier Trono (Addgene plasmid, #12260; http://n2t.net/addgene, 12260; RRID, Addgene_12260). VSV-G envelope-expressing plasmid pMD2.G was a gift from Didier Trono (Addgene plasmid, #12259; http://n2t.net/addgene, 12259; RRID, Addgene_12259).

Clustered regularly interspaced short palindromic repeats (CRISPR)/CRISPR-associated protein 9 (Cas9)-mediated genome editing of Jurkat cells

XXYLT1 knockout (KO) Jurkat cells were generated as previously described.[25] The pX330-Cas9-mEGFP vector was kindly provided by Drs Yusuke Maeda and Taroh Kinoshita.[33] The guide RNA sequence targeting *XXYLT1* Exon 1:5′-TAACCTTCACTTCGTGAGCG-3′ (gRNA-1) or 5′-CGCCAAGTTCGAGGCGCACG-3′ (gRNA-3) were inserted into the Bbs I site of pX330-Cas9-mEGFP. A total of 2.0×10^5/mL of Jurkat cells grown in a 60-mm culture dish was transfected with 11 μg of Cas9 and gRNA expression plasmid using Lipofectamine 3000 (Thermo Fisher Scientific). After transfection, the EGFP-positive Jurkat cells were sorted into individual wells of a 96-well plate using a FACS SORP Aria II flow cytometer (BD Biosciences, Franklin Lakes, NJ, USA). Successful gene editing was confirmed by genomic PCR using KOD FX-Neo polymerase and subsequent DNA sequencing.

Site-mapping of O-glucose glycans on the extracellular domain of NOTCH1 proteins by mass spectrometry

Totals of 2.0×10^5 Jurkat cells were cultured in eight 100 mm dishes with 10 mL of RPMI 1640 medium (Gibco) supplemented with 10% FBS. The cells were transiently transfected with 28 μg/dish of pSecTag2c-mouse NOTCH1 EGF8-12-Myc-His_6 plasmid using Lipofectamine 3000 (Invitrogen). The next day, the medium was replaced with 6 mL of OPTI-MEM-I (Thermo Fisher Scientific), and the cells were cultured for another 2 days. Culture media were collected,

centrifuged, and filtered.

Samples were prepared as previously described.[25] Briefly, the NOTCH1 protein was purified using Ni-NTA agarose (FUJIFILM Wako). Purified proteins were reduced, alkylated, and separated by sodium dodecyl sulfate-polyacrylamide gel electrophoresis. The bands were visualized using GelCode Blue (Thermo Fisher Scientific), and they were excised and digested with trypsin. The digested (glyco)peptides were extracted from the gel, desalted, and enriched using a C18 Zip-Tip (Millipore).

Mass spectrometric analysis was performed using Orbitrap Fusion Tribrid Liquid Chromatography (LC)-mass spectrometer (Thermo Fisher Scientific). Precursor ion data were collected using an Orbitrap mass analyzer in the positive polarity mode within a range of m/z 400–1600 at a resolution of 2.4×10^5 with an Automatic Gain Control (AGC) target of 2.0×10^5. The conditions of LC and the method of higher-energy collision dissociation (HCD)-tandem mass spectrometry (MS/MS) fragmentation and fragment ion detection by linear ion-trap mass analyzer were set according to a previous study.[25]

As previously described,[34] the MS/MS spectra-based (glyco)peptide search was performed using Byonic v5.1.1 (Thermo Fisher Scientific). The peptide modification parameters are listed in Supplementary Table S1. Xcalibur v4.1 (Thermo Fisher Scientific) was utilized to generate extracted ion chromatograms (EICs) for all identified (glyco)peptides in the Byonic search. The assignment of each (glyco)peptide was validated using MS/MS spectra and the retention time of MS EICs.

Lentivirus vector production and transduction of Jurkat cells

HEK293T cells were seeded at 1.0×10^6 cells in 2.5 mL of medium per well in a 6-well plate. HEK293T cells were cultured for 24 h and then transfected with 2.5 μg of pLVX-M-puro (empty vector) or pLVX-M-human XXYLT1-HA-puro, 2.1 μg of psPAX2, and 1.4 μg of pMD2.G plasmid using 20 μg of PEI-MAX (Polysciences, Warrington, PA, USA). The cells were cultured for 6 h, and the culture medium was replaced with fresh DMEM-high glucose supplemented with 5% FBS, penicillin, and streptomycin. After 48 h, the culture medium was collected, centrifuged, and filtered through a 0.22 μm filter. A 500 μL volume of the viral supernatant was added to Jurkat cells that were seeded at 1.0×10^5 cells in 500 μL of medium per well in a 12-well plate. After incubation at 37 °C for 48 h, culture media were replaced with RPMI 1640 medium supplemented with 5% FBS, 1 mM sodium pyruvate, 2 mM GlutaMAX, 100 U/mL penicillin, 100 μg/mL streptomycin, and 1.0 μg/mL of puromycin (Thermo Fisher Scientific) for the antibiotic selection.

Flow cytometry-based NOTCH1 expression analysis

The endogenous levels of NOTCH1 on the cell surface of Jurkat clones were analyzed using a FACSCANTO II flow cytometer (BD Biosciences) as previously described.[25,35] Briefly, after washing Jurkat cells with flow cytometry buffer (Hank's Balanced Salt Solution [HBSS] containing 1% bovine serum albumin (BSA), 1 mM $CaCl_2$, and 0.02% NaN_3), the cells were incubated on ice with either 2 μg/mL of PE-conjugated anti-human NOTCH1 antibody (Clone, MHN1-519; BioLegend, San Diego, CA, USA) or PE-conjugated anti-mouse IgG1 antibody (Clone, MOPC-21; BioLegend) as an isotype control for 1 h. Subsequently, the cells were washed twice with 1 mL of flow cytometry buffer and analyzed using a FACSCANTO II flow cytometer (BD Biosciences). The gate was set using Forward Scatter (FSC) and Side Scatter (SSC) signals to collect 10,000 viable cells for each sample. Data analysis was performed using FlowJo v10.9.0 Software (BD Life Sciences).

Western blot-based NOTCH1 activation analysis

Totals of 2.5×10^5 cells of each Jurkat clone were seeded into 12-well plates and cultured at 37 °C under 5% CO_2. After 48 h, cells were collected and lysed using RIPA buffer containing a protease inhibitor cocktail (Roche, Basel, Switzerland). The protein concentration was calculated using the bicinchoninic acid assay (Thermo Fisher Scientific). Total cell lysates (5 μg) were loaded and subsequently analyzed by western blotting using anti-αTubulin antibody (DSHB, 12G10, 1:4000), anti-cleaved NOTCH1 (Val1744) antibody (CST, D3B8, 1:1000), and anti-HA antibody (MBL, 561, 1:1000), and the intensity of cleaved NOTCH1 was normalized to the intensity of αTubulin.

Cell proliferation assay

Totals of 5.0×10^3 cells of each Jurkat clone in 100 μL of culture medium were seeded into 96-well plates and cultured at 37 °C under 5% CO_2. After 72 h, 10 μL of Cell Counting Kit-8 (CCK-8) solution (DOJINDO, Kumamoto, Japan) was added to each well, and cells were incubated at 37 °C under 5% CO_2 for 4 h. Absorbance was measured at 450 nm using a SpectraMax iD5 (Molecular Devices, San Jose, CA, USA).

Quantitative reverse transcription PCR analysis

Totals of 2.5×10^5 cells of each Jurkat clone were seeded into 12-well plates and cultured for 48 h. For the gamma-secretase inhibition experiment, Jurkat cells were cultured under 10 μM of N-[2S-(3, 5-difluorophenyl) acetyl]-L-alanyl-2-phenyl-glycine, 1, 1-dimethylethyl ester ([DAPT] Cayman Chemical, Ann Arbor, USA) diluted in Dimethyl Sulfoxide ([DMSO]; FUJIFILM Wako) or an equivalent concentration of DMSO. Total RNA was isolated using TRIzol (Thermo Fisher Scientific) and subsequently subjected to reverse transcription using the ReverTra Ace qPCR RT Master Mix with gDNA Remover (TOYOBO) following the manufacturer's protocol. Real-time PCR reactions were performed with SsoAdvanced Universal SYBR Green Supermix (BIO-RAD, Hercules, CA, USA) using primers: 5′-ACTTCAACAGCGACACCCAC-3′ and 5′-CAACTGTGAGGAGGGGAGAT-3′ for *GAPDH*, and 5′-GGGTAGTGGAAAACCAGCCTC-3′ and 5′-AGAAATACGGCTGCACCGAG-3′ for *MYC*. Relative expression levels were calculated by the double-delta CT method using the Ct value of *GAPDH* as a control and normalized to the *MYC* expression levels in wild-type cells transduced with an empty lentiviral vector.

Data analysis and statistics

Statistical analyses were performed using the R Studio software v2024.04.2+764 (Posit). Significance was tested using the Student's t-test or one-way analysis of variance (ANOVA) with Dunnett's comparison or Tukey's multiple comparison test as indicated in the figure legends.

RESULTS

O-Glucose on NOTCH1 EGF repeats overexpressed in Jurkat cells is xylosyl elongated

To begin to address the role of *XXYLT1* in Jurkat cells, we first investigated if XXYLT1 is enzymatically functional in Jurkat cells by examining whether glycoproteins derived from Jurkat cells are modified with the *O*-Glc trisaccharide Xyl-Xyl-Glc as previously performed with another cell line (eg, HEK293T cells) with a different lineage.[20,25,36,37] EGF8-12 of NOTCH1 with C-terminal $MycHis_6$ was transiently expressed in Jurkat cells, purified, digested with trypsin, and analyzed by LC-MS/MS. We successfully identified a triply charged glycopeptide (m/z 1253.8589) carrying an *O*-Glc trisaccharide derived from EGF10 of NOTCH1 (Figure 1A). The sequential

neutral loss of two pentose residues and one hexose residue supports the linear structure of the glycan modification of this peptide. Glycopeptides carrying other glycoforms of *O*-Glc were also identified (Figure S1). EICs exhibiting the sum of the relative intensities of triply and quadrivalent charged ions derived from peptides carrying each identified glycoform confirmed that, similar to what we observed in HEK293T cells, the Xyl-Xyl-Glc trisaccharide was the most abundant glycoform of *O*-Glc on EGF10 in Jurkat cells (Figure 1B).[25] These data confirm the rationality of our investigation into the role of EGF xylosylation in Jurkat cells. We then generated *XXYLT1* KO Jurkat clones using CRISPR-Cas9 technology. Genomic DNA sequencing analyses of single-cell-sorted clones confirmed the disruption of *XXYLT1* coding sequence in five clones (Figure S2). To verify that XXYLT1 is the sole enzyme that catalyzes the addition of terminal Xyl to *O*-Glc disaccharides, we selected one clone from each of the different gRNA-targeted clones (ID: KO #1 from gRNA-3 and KO #3 from gRNA-1) and performed the same MS analysis of the overexpressed NOTCH1 fragments, including those derived from a control clone. NOTCH1 EGF8-12 produced in both *XXYLT1* KO Jurkat clones exhibited a complete loss of the terminal Xyl on *O*-Glc, suggesting that XXYLT1 is the sole enzyme that transfers the terminal Xyl residue to Xyl-Glc-*O*-Ser in Jurkat cells (Figure 1C–E, Figure S3–5).

XXYLT1 inhibits NOTCH1 activation in Jurkat cells

Jurkat cells have been reported to possess a juxtamembrane-expanding mutation of *NOTCH1*, and this leads to the constitutive activation of NOTCH1 independently of ligands.[30] A previous study demonstrated that the knockdown of *POGLUT1* leads to impaired NOTCH1 activation in Jurkat cells.[38] We investigated whether *XXYLT1* upregulated or downregulated NOTCH1 activation in Jurkat cells by western blotting with an antibody against activated NOTCH1 (Val1744). Interestingly, deletion of *XXYLT1* in Jurkat cells increased the expression of activated NOTCH1 (Figure 2A, B). To exclude any Cas9 off-target effects, the *XXYLT1* KO clone (ID: KO #3) was transduced with a lentivirus vector expressing human XXYLT1 with a C-terminal HA tag and selected with puromycin. Indeed, NOTCH1 activation in *XXYLT1*-rescued *XXYLT1* KO cells was downregulated to a level comparable to that in wild-type cells (Figure 2C, D). These data support the hypothesis that *XXYLT1* inhibits NOTCH1 activation in Jurkat cells.

Previously, we demonstrated that the cell surface expression of endogenous NOTCH1 was not altered, but the cell surface expression of overexpressed NOTCH1 was impaired in *XXYLT1* KO HEK293T cells when compared to that in wild-type control cells.[25] In contrast, in flies it was demonstrated that the loss of xylosylation increased the cell surface abundance of Notch in the specific context.[22] We then wondered whether the observed enhancement of NOTCH1 activation in *XXYLT1* KO Jurkat clones depended on the cell surface expression of NOTCH1. To answer this question, we performed a flow cytometric analysis of endogenous NOTCH1 expressed in each Jurkat clone. As observed in HEK293T cells, the cell surface NOTCH1 levels in *XXYLT1* KO clones were comparable to those in wild-type and control clones (Figure 2E), thus indicating that XXYLT1 is dispensable for the cell surface expression of endogenous NOTCH1. Thus, these data suggest that the loss of *XXYLT1* affects the Notch activation process(es) after proper trafficking of NOTCH1 to the cell surface membrane.

Loss of XXYLT1 impairs the proliferation of Jurkat cells

Next, we investigated if *XXYLT1* regulates Jurkat cell proliferation. We examined the proliferation of *XXYLT1* KO clones (ID: KO #3) transduced with an empty vector or *XXYLT1* in addition to wild-type Jurkat cells transduced with an empty vector or *XXYLT1* using the CCK-8. After culturing for 72 h, cell growth was significantly impaired in *XXYLT1* KO cells transduced with the empty vector compared to wild-type cells transduced with the empty vector (control;

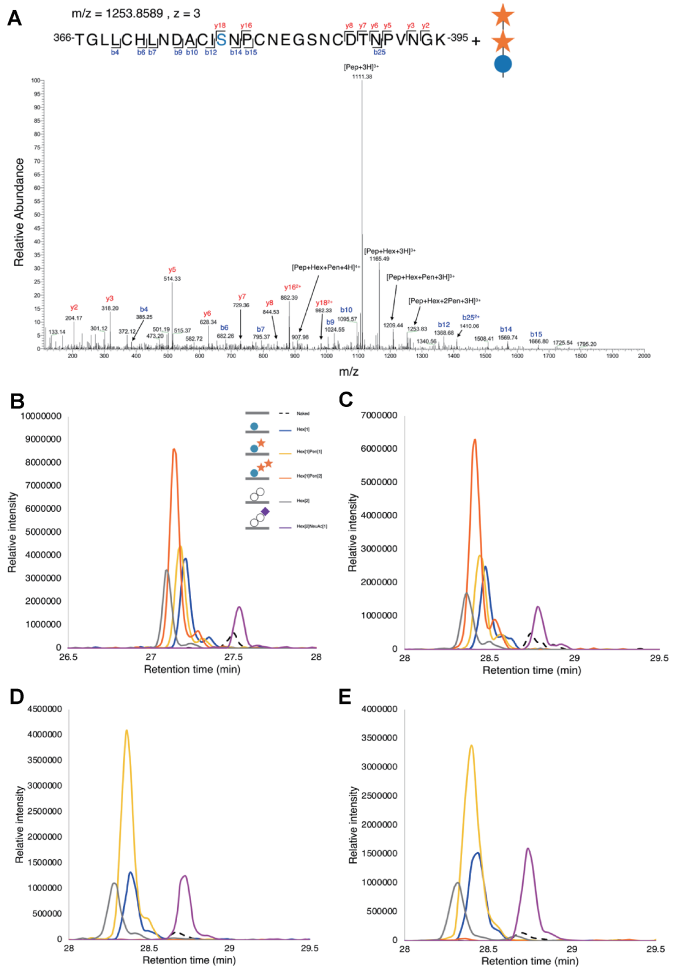

Fig. 1 NOTCH1 EGF repeats overexpressed in Jurkat cells are modified with the *O*-glucose trisaccharide at EGF10

Fig. 1A: HCD-MS/MS spectra of a glycopeptide from NOTCH1EGF10 carrying the *O*-Glc trisaccharide Xyl-Xyl-Glc. Numerous b and y ions in addition to the sequential neutral loss of sugar residues from the precursor ion confirm the identity of the peptide and the presence of the *O*-Glc trisaccharide.

Fig. 1B–E: EICs of glycopeptides from EGF10 modified with previously reported glycoforms. Blue circles, glucose; Orange stars, Xyl; White circles, uncharacterized hexose; Black dashed line, naked peptide; Blue, peptide + *O*-Glc; Yellow, peptide + *O*-Glc-Xyl; Orange, peptide + *O*-Glc-Xyl-Xyl; Gray, peptide + 2 hexoses; Purple, peptide + 2 hexoses and sialic acid. (B) WT Jurkat cells, (C) Cas9 control cells, (D) *XXYLT1* KO #1 (gRNA-3 transfectant), and (E) *XXYLT1* KO #3 (gRNA-1 transfectant).

EGF: epidermal growth factor-like
HCD: higher-energy collision dissociation
MS/MS: tandem mass spectrometry
Glc: glucose
Xyl: xylose
EICs: extracted ion chromatograms
WT: wild-type
Cas9: CRISPR-associated protein 9
XXYLT1: xyloside α1-3xylosyltransferase 1
KO: knockout
gRNA: guide RNA

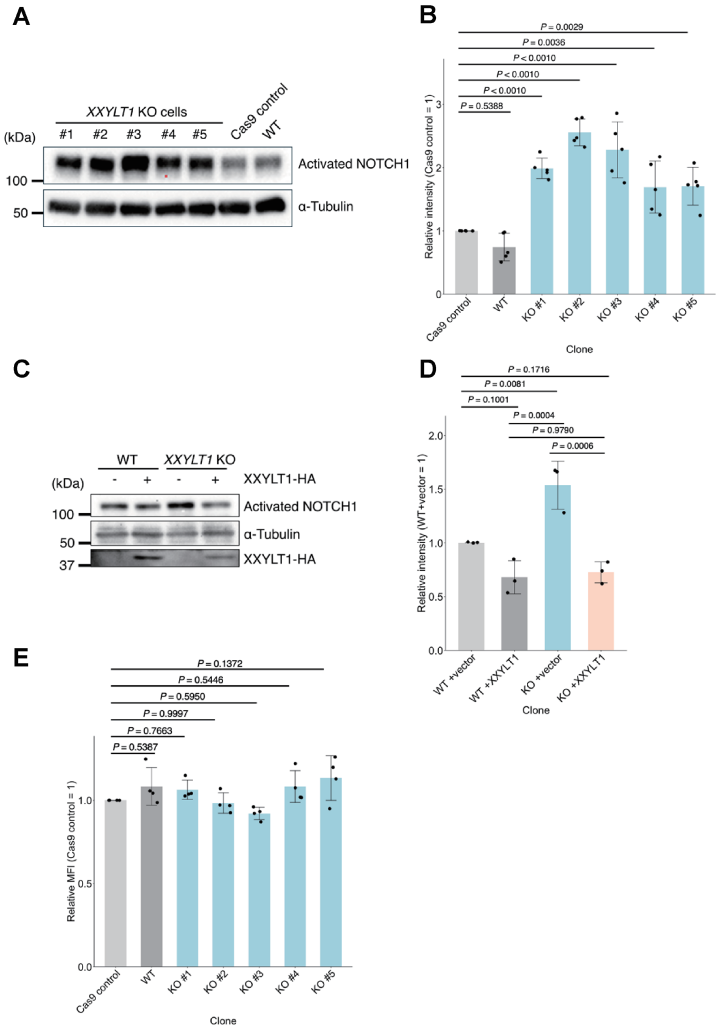

Fig. 2 The activation of NOTCH1 is enhanced in *XXYLT1* KO Jurkat clones

Fig. 2A: Western Blot analysis of WT, Cas9-control, and *XXYLT1* KO clones using antibodies against activated NOTCH1 (Val1744) and α-tubulin (loading control).

Fig. 2B: Normalized intensities of activated NOTCH1 signals from five independent experiments. Error bars indicate standard deviation. Significance was calculated using a one-way ANOVA followed by Dunnett's test.

Fig. 2C: Western Blot analysis of NOTCH1 activation in empty vector or *XXYLT1-HA*-transduced WT and *XXYLT1* KO cells.

Fig. 2D: Normalized intensities of activated NOTCH1 signals from three independent experiments. Error bars indicate standard deviation. Significance was calculated using a one-way ANOVA followed by Tukey's test.

Fig. 2E: Flow cytometry analysis of cell surface NOTCH1 in WT, Cas9-control, and *XXYLT1* KO clones. Normalized mean fluorescence intensities from four independent experiments were plotted. Error bars represent the standard deviation. Significance was calculated using a one-way ANOVA followed by Dunnett's test.

XXYLT1: xyloside α1-3xylosyltransferase 1
KO: knockout
WT: wild-type
Cas9: CRISPR-associated protein 9
ANOVA: analysis of variance
HA: hemagglutinin tag
MFI: mean fluorescence intensity

Figure 3). Moreover, *XXYLT1*-transduced cells exhibited enhanced proliferation in both wild-type and *XXYLT1* KO backgrounds compared to that of empty vector-transduced cells, although the transduction of *XXYLT1-HA* in *XXYLT1* KO cells did not fully rescue proliferation. These data indicated that *XXYLT1* positively regulates Jurkat cell proliferation.

MYC is downregulated in XXYLT1 KO cells

Palomero et al reported that *MYC*, a well-known and crucial regulator of cell proliferation, is a target of NOTCH1 target genes.[39,40] We examined *MYC* expression in wild-type Jurkat cells after treatment with DAPT, an inhibitor of the gamma-secretase complex. As previously reported,[41] *MYC* expression was downregulated in DAPT-treated Jurkat cells compared to that in DMSO-treated control cells (Figure 4A). Next, we assessed the transcriptional expression of *MYC* in each Jurkat clone. Here again, although enhanced NOTCH1 activation was observed in *XXYLT1* KO cells, the expression level of *MYC* was downregulated in *XXYLT1* KO cells and rescued in *XXYLT1-HA* transduced-*XXYLT1* KO cells (Figure 4B). These results suggest that *XXYLT1* regulates *MYC* expression via NOTCH1-independent pathways and promotes Jurkat cell proliferation.

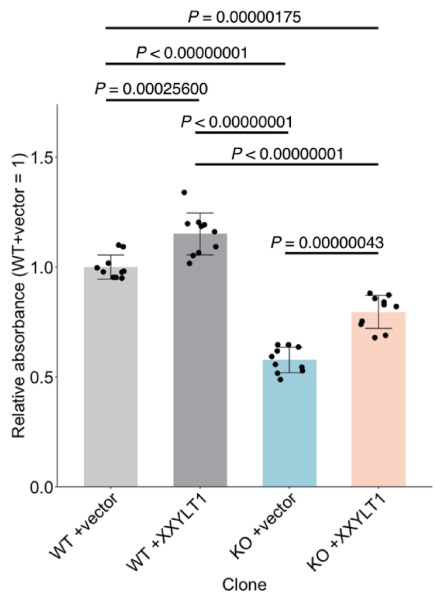

Fig. 3 Cell proliferation of *XXYLT1* KO Jurkat cells is impaired

The proliferation of Jurkat clones was evaluated using the CCK-8 assay after culturing for 72 h. Absorbance at 450 nm was normalized to that of WT Jurkat cells transduced with an empty vector. Data were obtained from two independent experiments with five technical replicates. Error bars represent the standard deviation. Significant differences were calculated using one-way ANOVA followed by Tukey's test.

XXYLT1: xyloside α1-3xylosyltransferase 1

KO: knockout

CCK-8: Cell Counting Kit-8

WT: wild-type

ANOVA: analysis of variance

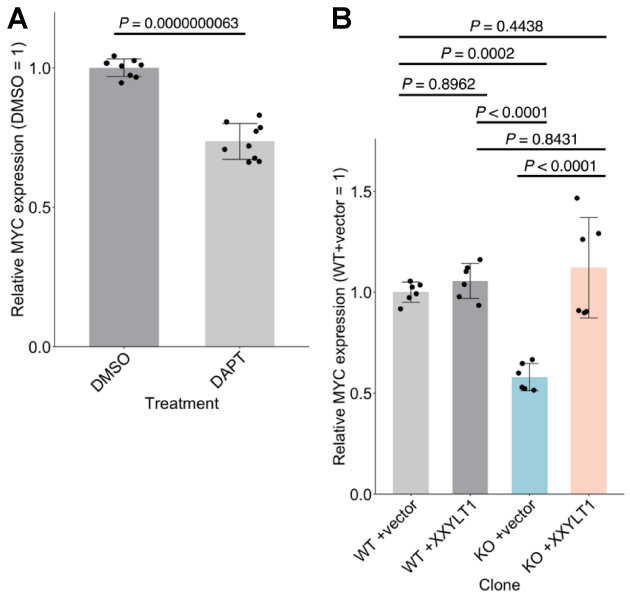

Fig. 4 Transcriptional expression of *MYC* is downregulated in *XXYLT1* KO cells

Fig. 4A: qRT-PCR analysis of *MYC* expression normalized to *GAPDH* was performed after culturing WT Jurkat cells with DMSO or DAPT for 48 h. Data were obtained from nine technical replicates. Error bars represent the standard deviation. Significant differences were calculated using the Student's t-test.

Fig. 4B: qRT-PCR analysis of *MYC* expression normalized to *GAPDH* in WT or *XXYLT1* KO cells transduced with empty vector or *XXYLT1-HA*. The plots represent relative values from two independent experiments with three technical replicates. Error bars represent the standard deviation. Significant differences were calculated using one-way ANOVA followed by Tukey's test.

XXYLT1: xyloside α1-3xylosyltransferase 1
KO: knockout
DMSO: dimethyl sulfoxide
DAPT: N-[2S-(3, 5-difluorophenyl) acetyl]-L-alanyl-2-phenyl-glycine, 1, 1-dimethylethyl ester
WT: wild-type
ANOVA: analysis of variance
qRT-PCR: quantitative reverse transcription polymerase chain reaction

DISCUSSION

In this study, we demonstrated that deletion of *XXYLT1* in Jurkat cells leads to enhanced NOTCH1 activation, suggesting that terminal Xyl inhibits ligand-independent NOTCH1 activation in Jurkat cells. In a previous study, Ma et al demonstrated that the knockdown of *POGLUT1* that encodes the protein *O*-glucosyltransferase that catalyzes the addition of *O*-Glc to EGF domains results in impaired NOTCH1 activation in Jurkat cells.[38] Based on this and our latest findings, *O*-glucosylation and xylosylation work in opposite directions in Jurkat cells in a manner similar to that observed in *Drosophila*.[22-24] The observation that terminal Xyl residues mildly affect Notch activation in *Drosophila* is consistent with the mass spectrometric analysis of *Drosophila* Notch in S2 cells that exhibited a limited level of Notch xylosylation.[42]

Recent cancer genome analyses have identified several Notch-related mutations, suggesting the involvement of Notch signaling in cancers.[26] As previously we reported, *XXYLT1* is frequently amplified in certain types of cancers.[43] Additionally, the upregulation of *XXYLT1* messenger RNA (mRNA) expression contributes to the genomic signature of head and neck squamous cell

carcinoma,[44] where NOTCH1 is frequently reported to be inactivated.[45] Our study deepens the understanding of Notch regulation by glycosylation and suggests the potential involvement of *XXYLT1* in carcinogenesis. However, if the effects of *XXYLT1* are similar in ligand-dependent NOTCH1 activation and other types of ligand-independent activation remains unclear. Lunatic Fringe (LFNG), another enzyme responsible for the elongation of *O*-Fuc, has been reported to unalter ligand-independent NOTCH1 activation.[46] It is of interest how, on a molecular basis, *O*-Glc and xylosyl elongation are involved in S2 and S3 cleavage. Furthermore, the inhibition of XXYLT1 may be beneficial in other contexts that are more dependent upon NOTCH1 activation such as the production of chimeric antigen receptor (CAR) T cells, where NOTCH1 agonism is reported to enhance the anticancer activity of CAR-T cells.[47,48]

Despite the enhanced activation of NOTCH1, cell proliferation and transcriptional expression of the *MYC* gene were unexpectedly downregulated in *XXYLT1* KO Jurkat cells. Interestingly, in endothelial cells, hyperactivation of NOTCH1 has been reported to repress *MYC* expression by microRNA-218.[49] In contrast to extensive studies examining the inhibition of Notch in T-ALL cell lines, there is a lack of literature focused on the consequences of further activation of NOTCH1 in T-ALL cells. In T cells, the intracellular domain of NOTCH1 has been shown to interact with NF-κB and repress the transcription of NF-κB target genes.[50] As NF-κB inhibition is generally associated with induction of apoptosis, enhanced NOTCH1 activation may affect cell growth via apoptotic regulation. Nevertheless, we cannot conclude that our observations are related to NOTCH1 hyperactivation.

These findings also suggest that XXYLT1 is critical for substrates other than NOTCH1 in Jurkat cells. The NOTCH3-JAG1 axis, for example, is reported to be involved in the pathogenesis of T-ALL.[51-54] Jurkat cells express JAG1.[55] Given that POGLUT1-mediated *O*-glucosylation inhibits JAG1 function in the liver,[56,57] XXYLT1 may be important for the complete function of JAG1. These issues must be addressed in future studies.

AUTHOR CONTRIBUTIONS

W.W. and W.S. contributed equally as co-first authors to this work. W.W., T.O., and H.T. designed the study. W.W. and H.T. established *XXYLT1* KO Jurkat clones. W.W., W.S., Y.T., T.O., and H.T. performed the mass spectrometric analysis of the glycoproteins from Jurkat cells. W.W., W.S., S.U., and Y.K. performed the cell biology experiments. W.W., W.S., T.O., and H.T. analyzed the data. W.S., W.W., and H.T. prepared the initial draft of the manuscript. All authors have approved the final manuscript.

CONFLICTS OF INTEREST

The authors declare no conflicts of interest for this article.

FUNDING

This work was supported by research grants from the Daiichi Sankyo Foundation of Life Science and Mizutani Glycoscience Foundation to H.T., JSPS KAKENHI Grant Numbers 23KJ1062 to Y.T., JP17H06743, JP19KK0195, and JP19H03176 to H.T., JP19H03416 and 23K24077 to T.O. and JST SPRING #JPMJSP2125 to W.W.

ACKNOWLEDGMENTS

We thank Messrs. Minoru Tanaka and Kentaro Taki at the Division for Medical Research Engineering, Nagoya University Graduate School of Medicine, for assisting with flow cytometry-mediated single-cell sorting and mass spectrometric analysis, respectively, Drs. Yuji Suzuki and Kazuma Sakamoto (Nagoya University) for their helpful advice regarding cell proliferation assays, and Dr. Koichi Furukawa (Chubu University) for generously providing Jurkat cells. We are also grateful to the members of the Okajima and Takeuchi laboratories for their critical comments and technical support.

MISCELLANEOUS ACKNOWLEDGMENTS

This work was supported by Nagoya University CIBoG WISE program from MEXT to W.S., and W.W. would like to take this opportunity to acknowledge the "Interdisciplinary Frontier Next-Generation Researcher Program of the Tokai Higher Education and Research System". We thank Editage (www.editage.jp) for English language editing.

REFERENCES

1 Uy R, Wold F. Posttranslational Covalent Modification of Proteins. *Science*. 1977;198(4320):890–896. doi:10.1126/science.337487
2 Haltiwanger RS, Lowe JB. Role of glycosylation in development. *Annu Rev Biochem*. 2004;73:491–537. doi:10.1146/annurev.biochem.73.011303.074043
3 Reily C, Stewart TJ, Renfrow MB, Novak J. Glycosylation in health and disease. *Nat Rev Nephrol*. 2019;15(6):346–366. doi:10.1038/s41581-019-0129-4
4 Stanley P. Genetics of glycosylation in mammalian development and disease. *Nat Rev Genet*. 2024;25(10):715–729. doi:10.1038/s41576-024-00725-x
5 Takeuchi H, Haltiwanger RS. Significance of glycosylation in Notch signaling. *Biochem Biophys Res Commun*. 2014;453(2):235–242. doi:10.1016/j.bbrc.2014.05.115
6 Varshney S, Stanley P. Multiple Roles for O-Glycans in Notch Signalling. *FEBS Lett*. 2018;592(23):3819–3834. doi:10.1002/1873-3468.13251
7 Pandey A, Niknejad N, Jafar-Nejad H. Multifaceted regulation of Notch signaling by glycosylation. *Glycobiology*. 2021;31(1):8–28. doi:10.1093/glycob/cwaa049
8 Saiki W, Ma C, Okajima T, Takeuchi H. Current Views on The Roles of O-Glycosylation in Controlling Notch-ligand Interactions. *Biomolecules*. 2021;11(2):309. doi:10.3390/biom11020309
9 Okajima T, Irvine KD. Regulation of Notch Signaling by O-Linked Fucose. *Cell*. 2002;111(6):893–904. doi:10.1016/S0092-8674(02)01114-5
10 Shi S, Stanley P. Protein O -fucosyltransferase 1 is an essential component of Notch signaling pathways. *Proc Natl Acad Sci U S A*. 2003;100(9):5234–5239. doi:10.1073/pnas.0831126100
11 Acar M, Jafar-Nejad H, Takeuchi H, et al. Rumi Is a CAP10 Domain Glycosyltransferase that Modifies Notch and Is Required for Notch Signaling. *Cell*. 2008;132(2):247–258. doi:10.1016/j.cell.2007.12.016
12 Fernandez-Valdivia R, Takeuchi H, Samarghandi A, et al. Regulation of mammalian Notch signaling and embryonic development by the protein O-glucosyltransferase Rumi. *Development*. 2011;138(10):1925–1934. doi:10.1242/dev.060020
13 Yu H, Takeuchi H. Protein O-glucosylation: another essential role of glucose in biology. *Curr Opin Struct Biol*. 2019;56:64–71. doi:10.1016/j.sbi.2018.12.001
14 Taylor P, Takeuchi H, Sheppard D, et al. Fringe-mediated extension of O -linked fucose in the ligand-binding region of Notch1 increases binding to mammalian Notch ligands. *Proc Natl Acad Sci U S A*. 2014;111(20):7290–7295. doi:10.1073/pnas.1319683111
15 Kakuda S, Haltiwanger RS. Deciphering the Fringe-Mediated Notch Code: Identification of Activating and Inhibiting Sites Allowing Discrimination between Ligands. *Dev Cell*. 2017;40(2):193–201. doi:10.1016/j.devcel.2016.12.013

16 Pandey A, Harvey BM, Lopez MF, Ito A, Haltiwanger RS, Jafar-Nejad H. Glycosylation of Specific Notch EGF Repeats by O-Fut1 and Fringe Regulates Notch Signaling in Drosophila. *Cell Rep*. 2019;29(7):2054–2066.e6. doi:10.1016/j.celrep.2019.10.027
17 Kakuda S, LoPilato RK, Ito A, Haltiwanger RS. Canonical Notch ligands and Fringes have distinct effects on NOTCH1 and NOTCH2. *J Biol Chem*. 2020;295(43):14710–14722. doi:10.1074/jbc.ra120.014407
18 Sethi MK, Buettner FF, Krylov VB, et al. Identification of glycosyltransferase 8 family members as xylosyltransferases acting on O-glucosylated Notch epidermal growth factor repeats. *J Biol Chem*. 2010;285(3):1582–1586. doi:10.1074/jbc.C109.065409
19 Sethi MK, Buettner FF, Ashikov A, et al. Molecular cloning of a xylosyltransferase that transfers the second xylose to O-glucosylated epidermal growth factor repeats of notch. *J Biol Chem*. 2012;287(4):2739–2748. doi:10.1074/jbc.M111.302406
20 Rana NA, Nita-Lazar A, Takeuchi H, Kakuda S, Luther KB, Haltiwanger RS. O-glucose trisaccharide is present at high but variable stoichiometry at multiple sites on mouse Notch1. *J Biol Chem*. 2011;286(36):31623–31637. doi:10.1074/jbc.M111.268243
21 Takeuchi H, Kantharia J, Sethi MK, Bakker H, Haltiwanger RS. Site-specific O-glucosylation of the epidermal growth factor-like (EGF) repeats of notch: Efficiency of glycosylation is affected by proper folding and amino acid sequence of individual EGF repeats. *J Biol Chem*. 2012;287(41):33934–33944. doi:10.1074/jbc.M112.401315
22 Lee TV, Sethi MK, Leonardi J, et al. Negative Regulation of Notch Signaling by Xylose. *PLoS Genet*. 2013;9(6):e1003547. doi:10.1371/journal.pgen.1003547
23 Lee TV, Pandey A, Jafar-Nejad H. Xylosylation of the Notch receptor preserves the balance between its activation by trans-Delta and inhibition by cis-ligands in Drosophila. *PLoS Genet*. 2017;13(4):e1006723. doi:10.1371/journal.pgen.1006723
24 Pandey A, Li-Kroeger D, Sethi MK, et al. Sensitized genetic backgrounds reveal differential roles for EGF repeat xylosyltransferases in Drosophila Notch signaling. *Glycobiology*. 2018;28(11):849–859. doi:10.1093/glycob/cwy080
25 Urata Y, Saiki W, Tsukamoto Y, et al. Xylosyl Extension of O-Glucose Glycans on the Extracellular Domain of NOTCH1 and NOTCH2 Regulates Notch Cell Surface Trafficking. *Cells*. 2020;9(5):1220. doi:10.3390/cells9051220
26 Aster JC, Pear WS, Blacklow SC. The Varied Roles of Notch in Cancer. *Annu Rev Pathol*. 2017;12:245–275. doi:10.1146/annurev-pathol-052016-100127
27 Gianni F, Belver L, Ferrando A. The genetics and mechanisms of T-cell acute lymphoblastic leukemia. *Cold Spring Harb Perspect Med*. 2020;10(3):a035246. doi:10.1101/cshperspect.a035246
28 Ferrando AA. The role of NOTCH1 signaling in T-ALL. *Hematology Am Soc Hematol Educ Program*. 2009:353–361. doi:10.1182/asheducation-2009.1.353
29 Malecki MJ, Sanchez-Irizarry C, Mitchell JL, et al. Leukemia-Associated Mutations within the NOTCH1 Heterodimerization Domain Fall into at Least Two Distinct Mechanistic Classes. *Mol Cell Biol*. 2006;26(12):4642–4651. doi:10.1128/mcb.01655-05
30 Sulis ML, Williams O, Palomero T, et al. NOTCH1 extracellular juxtamembrane expansion mutations in T-ALL. *Blood*. 2008;112(3):733–740. doi:10.1182/blood-2007-12-130096
31 Hales EC, Orr SM, Gedman AL, Taub JW, Matherly LH. Notch1 receptor regulates AKT protein activation loop (Thr308) Dephosphorylation through modulation of the PP2A phosphatase in phosphatase and tensin homolog (PTEN)-null T-cell acute lymphoblastic leukemia cells. *J Biol Chem*. 2013;288(31):22836–22848. doi:10.1074/jbc.M113.451625
32 Zhang Y, Shi J, Liu X, et al. BAP1 links metabolic regulation of ferroptosis to tumour suppression. *Nat Cell Biol*. 2018;20(10):1181–1192. doi:10.1038/s41556-018-0178-0
33 Hirata T, Fujita M, Nakamura S, et al. Post-Golgi anterograde transport requires GARP-dependent endosome-to-TGN retrograde transport. *Mol Biol Cell*. 2015;26(17):3071–3084. doi:10.1091/mbc.E14-11-1568
34 Tsukamoto Y, Tsukamoto N, Saiki W, et al. Characterization of galactosyltransferase and sialyltransferase genes mediating the elongation of the extracellular O-GlcNAc glycans. *Biochem Biophys Res Commun*. 2024;703:149610. doi:10.1016/j.bbrc.2024.149610
35 Takeuchi H, Yu H, Hao H, et al. O-Glycosylation modulates the stability of epidermal growth factor-like repeats and thereby regulates Notch trafficking. *J Biol Chem*. 2017;292(38):15964–15973. doi:10.1074/jbc.M117.800102
36 Tsukamoto Y, Ogawa M, Yogi K, Tashima Y, Takeuchi H, Okajima T. Glycoproteomics of NOTCH1 EGF repeat fragments overexpressed with different glycosyltransferases in HEK293T cells reveals insights into O-GlcNAcylation of NOTCH1. *Glycobiology*. 2022;32(7):616–628. doi:10.1093/glycob/cwac015

37 Zhang A, Tsukamoto Y, Takeuchi H, Nishiwaki K, Tashima Y, Okajima T. Secretory expression of mammalian NOTCH tandem epidermal growth factor-like repeats based on increased O-glycosylation. *Anal Biochem*. 2022;656:114881. doi:10.1016/j.ab.2022.114881

38 Ma W, Du J, Chu Q, et al. HCLP46 regulates U937 cell proliferation via Notch signaling pathway. *Biochem Biophys Res Commun*. 2011;408(1):84–88. doi:10.1016/j.bbrc.2011.03.124

39 Palomero T, Lim WK, Odom DT, et al. NOTCH1 directly regulates c-MYC and activates a feed-forward-loop transcriptional network promoting leukemic cell growth. *Proc Natl Acad Sci U S A*. 2006;103(48):18261–18266. doi:10.1073/pnas.0606108103

40 Dhanasekaran R, Deutzmann A, Mahauad-Fernandez WD, Hansen AS, Gouw AM, Felsher DW. The MYC oncogene — the grand orchestrator of cancer growth and immune evasion. *Nat Rev Clin Oncol*. 2022;19(1):23–36. doi:10.1038/s41571-021-00549-2

41 Chadwick N, Zeef L, Portillo V, et al. Identification of novel Notch target genes in T cell leukaemia. *Mol Cancer*. 2009;8:35. doi:10.1186/1476-4598-8-35

42 Harvey BM, Rana NA, Moss H, Leonardi J, Jafar-Nejad H, Haltiwanger RS. Mapping sites of O-glycosylation and fringe elongation on Drosophila Notch. *J Biol Chem*. 2016;291(31):16348–16360. doi:10.1074/jbc.M116.732537

43 Yu H, Takeuchi M, LeBarron J, et al. Notch-modifying xylosyltransferase structures support an SNi-like retaining mechanism. *Nat Chem Biol*. 2015;11(11):847–854. doi:10.1038/nchembio.1927

44 Rodriguez E, Lindijer DV, van Vliet SJ, Garcia Vallejo JJ, van Kooyk Y. The transcriptional landscape of glycosylation-related genes in cancer. *iScience*. 2024;27(3):109037. doi:10.1016/j.isci.2024.109037

45 Agrawal N, Frederick MJ, Pickering CR, et al. Exome sequencing of head and neck squamous cell carcinoma reveals inactivating mutations in NOTCH1. *Science*. 2011;333(6046):1154–1157. doi:10.1126/science.1206923

46 Hicks C, Johnston SH, diSibio G, Collazo A, Vogt TF, Weinmaster G. Fringe differentially modulates Jagged1 and Delta1 signalling through Notch1 and Notch2. *Nat Cell Biol*. 2000;2(8):515–520. doi:10.1038/35019553

47 Wilkens AB, Fulton EC, Pont MJ, et al. NOTCH1 signaling during CD4+ T-cell activation alters transcription factor networks and enhances antigen responsiveness. *Blood*. 2022;140(21):2261–2275. doi:10.1182/blood.2021015144

48 Schneider M, Maillard I. Bumping CAR T cells up a Notch. *Blood*. 2022;140(21):2185–2186. doi:10.1182/blood.2022017055

49 Sun JX, Dou GR, Yang ZY, et al. Notch activation promotes endothelial quiescence by repressing MYC expression via miR-218. *Mol Ther Nucleic Acids*. 2021;25:554–566. doi:10.1016/j.omtn.2021.07.023

50 Wang J, Shelly L, Miele L, Boykins R, Norcross MA, Guan E. Human Notch-1 inhibits NF-kappa B activity in the nucleus through a direct interaction involving a novel domain. *J Immunol*. 2001;167(1):289–295. doi:10.4049/jimmunol.167.1.289

51 Bellavia D, Campese AF, Alesse E, et al. Constitutive activation of NF-kappaB and T-cell leukemia/lymphoma in Notch3 transgenic mice. *EMBO J*. 2000;19(13):3337–3348. doi:10.1093/emboj/19.13.3337

52 Minuzzo S, Agnusdei V, Pusceddu I, et al. DLL4 regulates NOTCH signaling and growth of T acute lymphoblastic leukemia cells in NOD/SCID mice. *Carcinogenesis*. 2015;36(1):115–121. doi:10.1093/carcin/bgu223

53 Choi SH, Severson E, Pear WS, Liu XS, Aster JC, Blacklow SC. The common oncogenomic program of NOTCH1 and NOTCH3 signaling in T-cell acute lymphoblastic leukemia. *PLoS One*. 2017;12(10):e0185762. doi:10.1371/journal.pone.0185762

54 Giuli MV, Diluvio G, Giuliani E, et al. Notch3 contributes to T-cell leukemia growth via regulation of the unfolded protein response. *Oncogenesis*. 2020;9(10):93. doi:10.1038/s41389-020-00279-7

55 Pelullo M, Quaranta R, Talora C, et al. Notch3/Jagged1 circuitry reinforces notch signaling and sustains T-ALL. *Neoplasia*. 2014;16(12):1007–1017. doi:10.1016/j.neo.2014.10.004

56 Thakurdas SM, Lopez MF, Kakuda S, et al. Jagged1 heterozygosity in mice results in a congenital cholangiopathy which is reversed by concomitant deletion of one copy of Poglut1 (Rumi). *Hepatology*. 2016;63(2):550–565. doi:10.1002/hep.28024

57 Niknejad N, Fox D, Burwinkel JL, et al. ASO silencing of a glycosyltransferase, Poglut1, improves the liver phenotypes in mouse models of Alagille syndrome. *Hepatology*. 2023;78(5):1337–1351. doi:10.1097/HEP.0000000000000380

SUPPLEMENTARY INFORMATION

Suppl Table S1 Summary of the parameters for the mass spectrometric analysis

Parameters	**Settings**
Cleavage sites	C-terminal of K, R
Digestion specificity	Fully specific
Number of allowed maximum miss cleavage	2
Precursor mass tolerance	20 ppm
Fragmentation type	QTOF/HCD
Fragment mass tolerance	0.5 Da

Maximum numbers of each fine control modifications on each peptide
Common: 2
Rare: 2

Modifications			
Fine control	Residue	Modification	Additional mass (Da)
Fixed	C	Carbamidomethylation	57.021464
Variable (common1)	D, M, N	Oxidation	15.994915
Variable (common1)	N-term C	Deamination	–17.026549

Glycans			
Fine control	Residue	Modification	Additional mass (Da)
Variable (rare1)	S, T	Hex(1)	162.053
Variable (rare1)	S, T	Hex(1)Pent(1)	294.095
Variable (rare1)	S, T	Hex(1)Pent(2)	426.137
Variable (rare1)	S, T	Hex(2)	324.106
Variable (rare1)	S, T	Hex(2)NeuAc(1)	615.201
Variable (rare1)	S, T	Fuc(1)	146.058
Variable (rare1)	S, T	HexNAc(1)Fuc(1)	349.137
Variable (rare1)	S, T	HexNAc(1)Hex(1)Fuc(1)	511.19
Variable (rare1)	S, T	HexNAc(1)Hex(1)Fuc(1)NeuAc(1)	802.286
Variable (rare1)	S, T	HexNAc(1)	203.079
Variable (rare1)	S, T	HexNAc(1)Hex(1)	365.132
Variable (rare1)	S, T	HexNAc(1)Hex(1)NeuAc(1)	656.228

The parameters included the cleavage sites, digestion specificity, number of allowed maximum missed cleavages, precursor mass tolerance, fragmentation type, and fragment mass tolerance. The additional masses and positions of the common modifications are carbamidomethylation, oxidation, and deamination. Additional masses and positions of the most common monosaccharides (HexNAc, Hex, Fuc, Pent, and NeuAc) are indicated.
K: lysine
R: arginine
ppm: parts per million
QTOF/HCD: quadrupole time-of-flight/ higher-energy collision dissociation
S: serine
T: threonine
Hex: hexose
Pent: pentose
NeuAc: *N*-acetylneuraminic acid
Fuc: fucose
HexNAc: *N*-acetylhexosamine

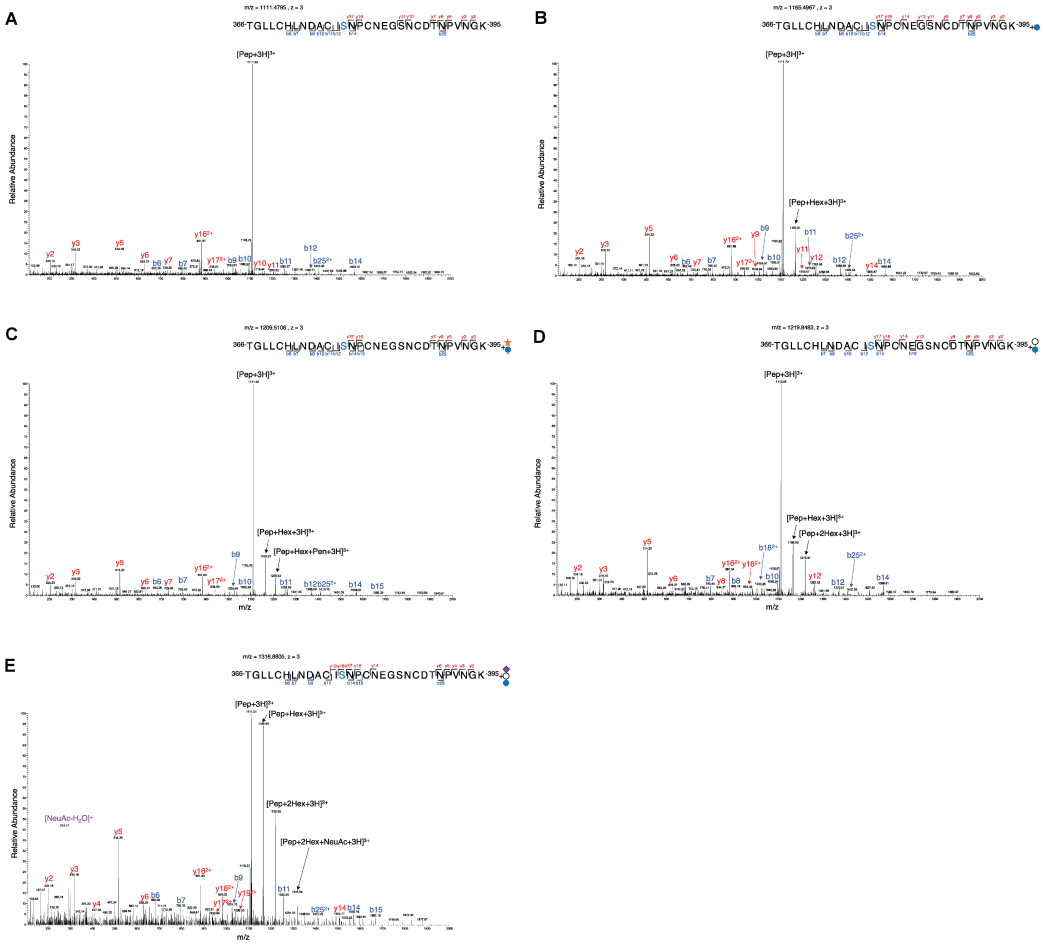

Fig. S1 Identification of glycopeptides carrying other glycoforms of *O*-Glc in wild-type Jurkat cells

HCD-MS/MS spectra of triply charged glycopeptides derived from EGF10 of NOTCH1. Samples were generated from WT Jurkat cells. The identity of the (glyco)peptides was confirmed based on the presence of peptide-specific b and y ions and the neutral loss of predicted glycans. The amino acid sequences and predicted glycans that include (A) none, (B) *O*-Glc, (C) *O*-Glc-Xyl, (D) *O*-Glc-hexose, and (E) *O*-Glc-hexose-sialic acid are presented along with the measured mass and charge states of the identified parental ions in the upper right corner. Blue, circle-glucose; orange, star-Xyl; white, circle-hexose; and purple, diamond-sialic acid.

HCD: higher-energy collision dissociation
MS/MS: tandem mass spectrometry
EGF: epidermal growth factor-like
WT: wild-type
Glc: glucose
Xyl: xylose

```
XXYLT1 KO#1:1-bp insertion (ALLELE1) or 151-bp insertion (ALLELE2) in XXYLT1
WT:       GCGCCTCGCCAAGTTCGAGGCGCACGAGGTGCT
ALLELE1: GCGCCTCGCCAAGTTTCGAGGCGCACGAGGTGCT
ALLELE2: GCGCCTCGCCAAGT*TCGAGGCGCACGAGGTGCT  (*151-bp-insertion)

XXYLT1 KO#2:1-bp insertion (ALLELE1) in XXYLT1
WT:       AGGTGCTTAACCTTCACTTCGTGAGCGAGGAGGCCA
ALLELE1: AGGTGCTTAACCTTCACTTCGTGAAGCGAGGAGGCCA

XXYLT1 KO#3:1-bp insertion (ALLELE1) or 2-bp insertion (ALLELE2) or 94-bp insertion (ALLELE3) in XXYLT1
WT:       AGGTGCTTAACCTTCACTTCGTGAGCGAGGAGGCCA
ALLELE1: AGGTGCTTAACCTTCACTTCGTGAAGCGAGGAGGCCA
ALLELE2: AGGTGCTTAACCTTCACTTCGTGAGGCGAGGAGGCCA
ALLELE3: AGGTGCTTAACCTTCACTTCGTGAG*CGAGGAGGCCA (*94-bp-insertion)

XXYLT1 KO#4:11-bp deletion (ALLELE1) or 38-bp deletion (ALLELE2) or 9-bp deletion (ALLELE3) in XXYLT1
WT:       AGGTGCTTAACCTTCACTTCGTGAGCGAGGAGGCCAGCCGCGAGGTGGCCAAGGGCCTGCTGCGGGA
ALLELE1: AGGTGCTTAACCTTCAC*GGAGGCCAGCCGCGAGGTGGCCAAGGGCCTGCTGCGGGA (*11-bp-deletion)
ALLELE2: AGGTGCTTAACCTTCACTTCGTG*GCGGGA (*38-bp-deletion)
ALLELE3: AGGTGCTTAACCTTCACTTCGTGA*CCAGCCGCGAGGTGGCCAAGGGCCTGCTGCGGGA (*9-bp-deletion)

XXYLT1 KO#5:1-bp insertion (ALLELE1) or 2-bp deletion (ALLELE2) or 19-bp deletion (ALLELE3) in XXYLT1
WT:       AGGTGCTTAACCTTCACTTCGTGAGCGAGGAGGCCAGCCGCGAGGTGGCCA
ALLELE1: AGGTGCTTAACCTTCACTTCGTGAAGCGAGGAGGCCAGCCGCGAGGTGGCCA
ALLELE2: AGGTGCTTAACCTTCACTTCG--AGCGAGGAGGCCAGCCGCGAGGTGGCCA
ALLELE3: AGGTGCTTAACCTTCACTTCGTG*AGGTGGCCA (*19-bp-deletion)
```

Fig. S2 Sequencing data of wild-type and *XXYLT1* KO Jurkat cells
Genomic sequences of the edited genomic regions in *XXYLT1* in WT Jurkat cells and corresponding KO clones. The gRNA sequences (TAACCTTCACTTCGTGAGCG and CGCCAAGTTCGAGGCGCACG) are underlined. Genomic DNA sequencing confirmed the disruption of the *XXYLT1* coding region and the generation of five KO clones.
XXYLT1: xyloside α1-3xylosyltransferase 1
WT: wild-type
KO: knockout
gRNA: guide RNA

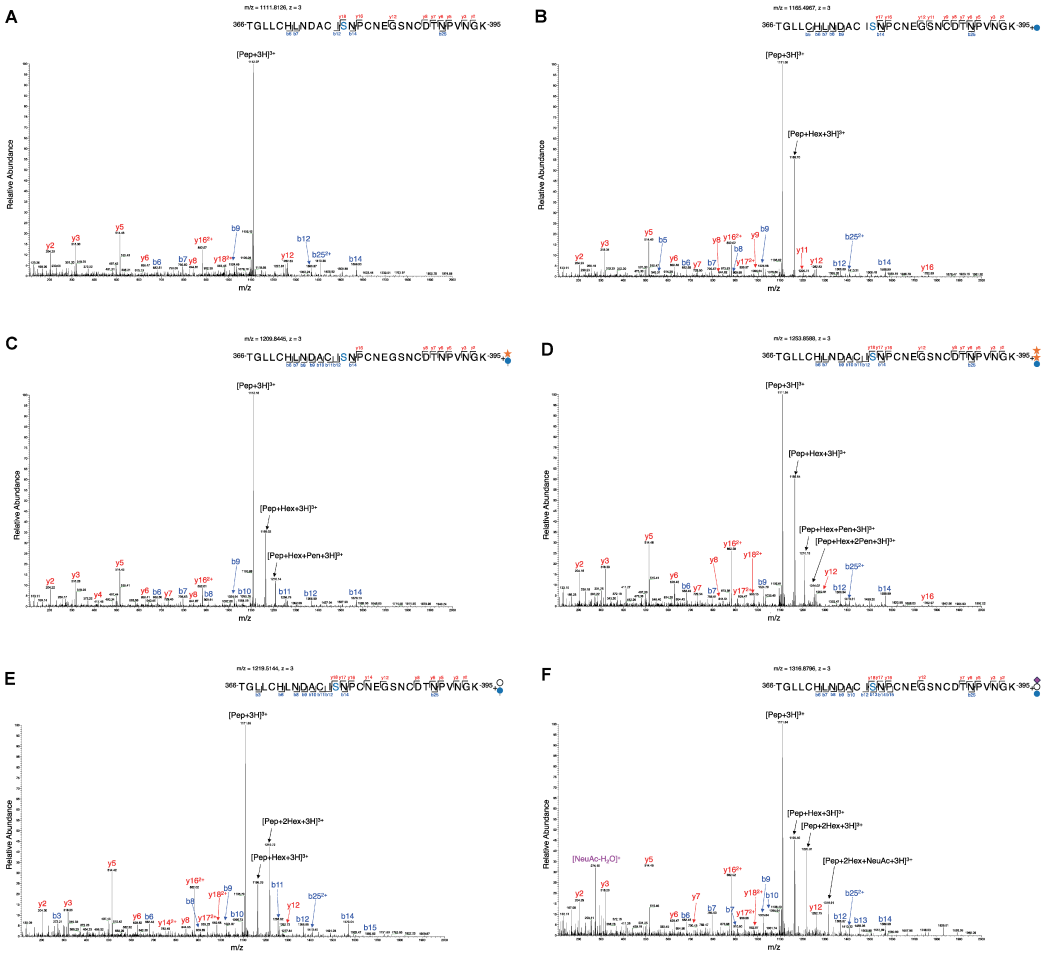

Fig. S3 Identification of glycopeptides carrying glycoforms of *O*-Glc in Cas9 control cells
HCD-MS/MS spectra of triply charged glycopeptides derived from EGF10 of NOTCH1. Samples were generated from the Cas9 control cells. The identity of the (glyco)peptides was confirmed based on the presence of peptide-specific b and y ions and the neutral loss of predicted glycans. The amino acid sequence and predicted glycans that include (A) none, (B) *O*-Glc, (C) *O*-Glc-Xyl, (D) *O*-Glc-Xyl-Xyl, (E) *O*-Glc-hexose, and (F) *O*-Glc-hexose-sialic acid are presented with the measured mass and charge state of the identified parental ions in the upper right corner. Blue, circle-glucose; orange, star-Xyl; white, circle-hexose; and purple, diamond-sialic acid.
HCD: higher-energy collision dissociation
MS/MS: tandem mass spectrometry
EGF: epidermal growth factor-like
Cas9: CRISPR-associated protein 9
Glc: glucose
Xyl: xylose

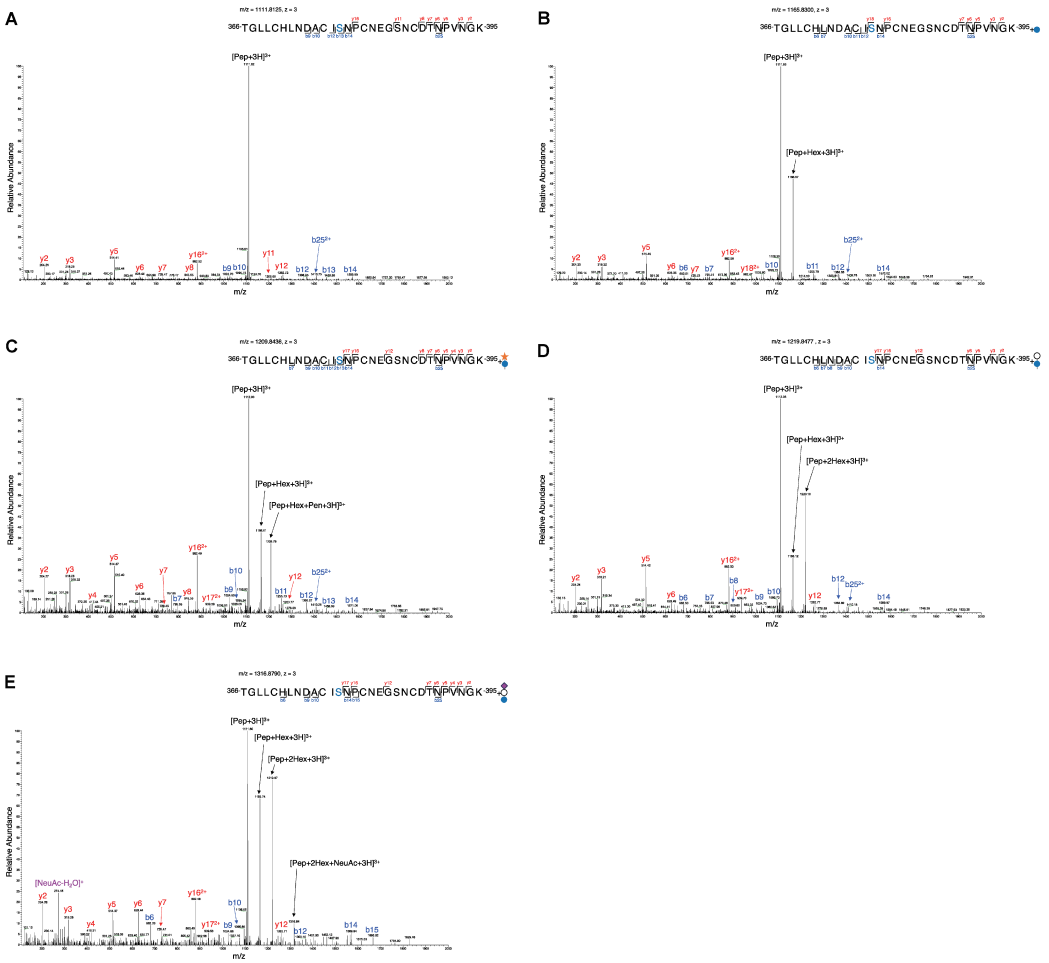

Fig. S4 Identification of glycopeptides carrying glycoforms of *O*-Glc in *XXYLT1* KO #1 Jurkat cells
HCD-MS/MS spectra of triply charged glycopeptides derived from EGF10 of NOTCH1. Samples were generated from *XXYLT1* KO #1 Jurkat cells (transfected with gRNA-3). The identity of the (glyco)peptides was confirmed based on the presence of peptide-specific b and y ions and the neutral loss of predicted glycans. The amino acid sequences and predicted glycans that include (A) none, (B) *O*-Glc, (C) *O*-Glc-Xyl, (D) *O*-Glc-hexose, and (E) *O*-Glc-hexose-sialic acid are presented along with the measured mass and charge states of the identified parental ions in the upper right corner. Blue, circle-glucose; orange, star-Xyl; white, circle-hexose; and purple, diamond-sialic acid.
XXYLT1: xyloside α1-3xylosyltransferase 1
KO: knockout
HCD: higher-energy collision dissociation
MS/MS: tandem mass spectrometry
EGF: epidermal growth factor-like
gRNA: guide RNA
Glc: glucose
Xyl: xylose

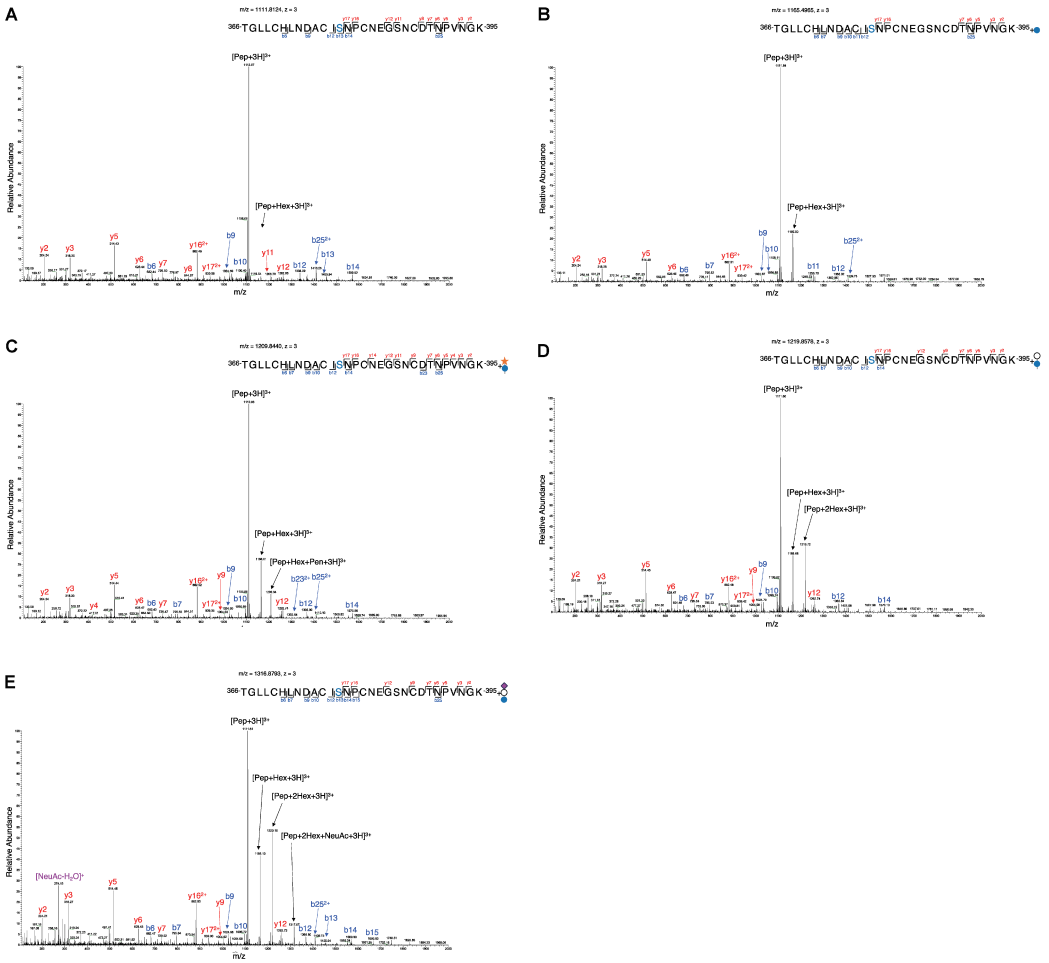

Fig. S5 Identification of glycopeptides carrying glycoforms of *O*-Glc in *XXYLT1* KO #3 Jurkat cells
HCD-MS/MS spectra of triply charged glycopeptides derived from EGF10 of NOTCH1. Samples were generated from *XXYLT1* KO #3 Jurkat cells (gRNA-1 transfectant). The identity of the (glyco)peptides was confirmed based on the presence of peptide-specific b and y ions and the neutral loss of predicted glycans. The amino acid sequences and predicted glycans that include (A) none, (B) *O*-Glc, (C) *O*-Glc-Xyl, (D) *O*-Glc-hexose, and (E) *O*-Glc-hexose-sialic acid are presented along with the measured mass and charge states of the identified parental ions in the upper right corner. Blue, circle-glucose; orange, star-Xyl; white, circle-hexose; and purple, diamond-sialic acid.

XXYLT1: xyloside α1-3xylosyltransferase 1
KO: knockout
HCD: higher-energy collision dissociation
MS/MS: tandem mass spectrometry
EGF: epidermal growth factor-like
gRNA: guide RNA
Glc: glucose
Xyl: xylose